City Research Online

City St George's, University of London

Citation: Reyes-Aldasoro, C. C., Barri, M. & Hafezparast, M. (2015). Automatic segmentation of focal adhesions from mouse embryonic fibroblasts. In: 2015 IEEE 12th International Symposium on Biomedical Imaging (ISBI). (pp. 548-551). IEEE. ISBN 9781479923748 doi: 10.1109/ISBI.2015.7163932

This is the accepted version of the paper.

This version of the publication may differ from the final published version. To cite this item please consult the publisher's version.

Permanent repository link: https://openaccess.city.ac.uk/id/eprint/12811/

Link to published version: https://doi.org/10.1109/ISBI.2015.7163932

Copyright and Reuse: Copyright and Moral Rights remain with the author(s) and/or copyright holders. Copies of full items can be used for personal research or study, educational, or not-for-profit purposes without prior permission or charge, unless otherwise indicated, provided that the authors, title and full bibliographic details are credited, a hyperlink and/or URL is given for the original metadata page and the content is not changed in any way. For full details of reuse please refer to City Research Online policy.

City Research Online: http://openaccess.city.ac.uk/ publications@citystgeorges.ac.uk

AUTOMATIC SEGMENTATION OF FOCAL ADHESIONS FROM MOUSE EMBRYONIC FIBROBLASTS

Constantino Carlos Reyes-Aldasoro[1], *Muruj Barri* [2], *Majid Hafezparast* [2]

1 Biomedical Engineering Research Centre, School of Mathematics, Computer Science and Engineering, City University London, London EC1V 0HB, UK
2 School of Life Sciences, University of Sussex, Brighton BN1 9QG, UK

ABSTRACT

This work describes an automatic algorithm for the segmentation and quantification of focal adhesions from mouse embryonic fibroblasts. The main challenges solved by this algorithm are: the variability of the intensity of the focal adhesions, the detection of an outer ring, which distinguishes the cell periphery responsible for the cell migration, and the quantification of the characteristics of the focal adhesions. The algorithm detects maximal regions through gradients and uses a region-growing algorithm limited by intensity-based edges. The outer ring is calculated based on the average radial intensity from an extended centroid of the cell. Finally, traditional morphological characteristics are obtained to distinguish between two groups of cells. Two of the measurements employed showed statistical difference between two groups of cells.

Index Terms— cell segmentation, mouse embryonic fibroblasts, MEF, focal adhesions.

1. INTRODUCTION

Focal adhesion formation at the leading edge of the cells and disassembly at the rear are crucial for the motility of many adhering cells. The formation of focal adhesions is initiated by the anchoring of F-actin to the intracellular domain of integrins via protein adaptors paxillin, talin, and vinculin. When F-actin anchors the lamellipodium to the attractant substrate, exploratory microtubules are thought to act as guidance sensors for further signaling and/or as scaffold for localized recruitment of key signaling components and additional recruitment of microtubules to the adhesion site. Focal adhesion formation and disassembly was analyzed by monitoring paxillin recruitment to the sites of adhesion as a means for profiling cell motility in relation to focal adhesion numbers and morphology. The recruitment of paxillin resulted in an increased intensity of the fluorescent marker at the areas of interest.

This paper describes an automatic methodology for the segmentation and quantification of the focal adhesions of mouse embryonic fibroblasts (MEFs), which were subjected to a cell-spreading assay. The algorithm detects the focal adhesions from the background by an intensity analysis by detecting local maxima, growing those regions with a stopping criterion determined by local edges. In addition, a region of interest (ROI) is determined for those focal adhesions that are located in the cell periphery, which is formed by the outer boundary of the cell and an outer ring of decreased intensity within the cell. Results of the algorithm are illustrated with 4 representative images extracted from two different groups.

2. MATERIALS AND METHODS

2.1. Materials

MEFs were cultured in Dulbecco's Modified Eagles Medium (DMEM) supplemented with 15% Hyclone (Fisher), 1% Penicillin/Streptomycin and 1% L-Glutamine. MEFs were cultured in a 37 degree C incubator with 3% O_2 and 5% CO_2. For analysis of focal adhesions, a cell-spreading assay was performed in which the MEFs were trypsinized, replated at low density and as a final step incubated for 1 hour (when most cells were spread). Cells were then fixed in 4% paraformaldehyde and stained with anti-paxillin antibody followed by imaging using a Delta Vision Core microscope (Applied precision). Fixed-cell images were captured in the FITC channel using a 40x oil/1.35 NA objective followed by deconvolution.

Two groups, labeled as A (n=16) and B (n=20) due to unpublished methodologies, were used to test the algorithm.

2.1. Segmentation algorithm

Red, green and blue channels of the images were separated and background and paxillin-stained focal adhesions on the green channel were separated with an Otsu threshold [1]. To obtain the external boundary of the cell from the thresholded foreground several steps were applied. The foreground was processed with a morphological closing with a circular structural element, holes were filled [2], and finally, connected components were labeled [3] so that only the largest object was kept and all small objects were removed. The calculation of the cell periphery where the focal adhesions of interest are located was based on the distance from a 'centroid' of the cell towards the boundary. Since the shapes of the cells can be irregular, a traditional centroid calculated as the geometric center would only be suitable for a regular circular cell.

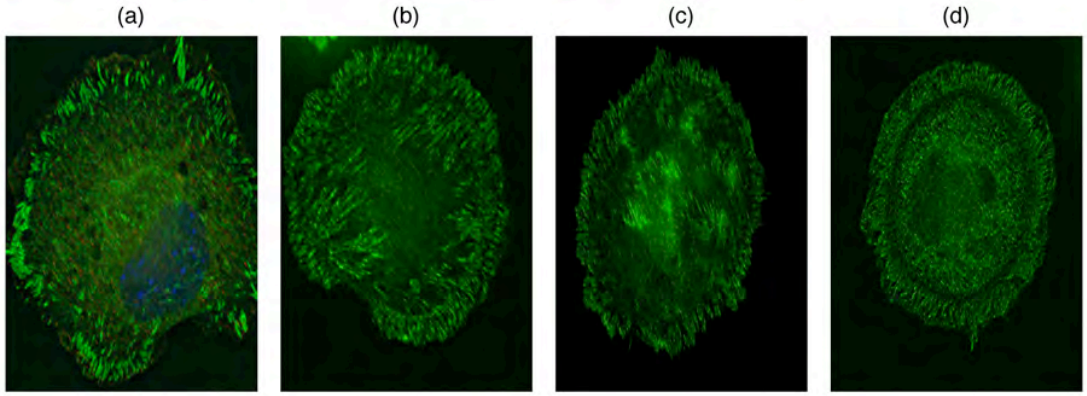

Fig. 1. Four representative images of MEFs on which a cell-spreading assay was performed. Notice the higher intensity of the paxillin-stained focal adhesions located towards the periphery of the cell. Notice as well a decreased intensity that forms an "outer ring", this is especially noticeable in (d).

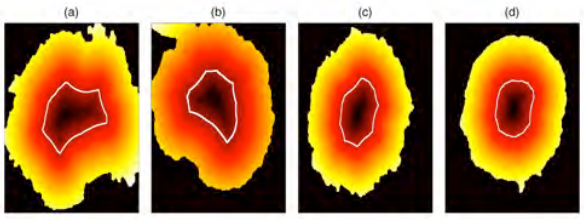

Fig. 2. The eroded shape that was used to replace a geometric centroid is displayed as a bright line within a Euclidean distance map from the external boundary of the cell.

To compensate for the irregularity of the cell shape, an irregular eroded version of the cell was obtained by calculating the Euclidean distance from the boundary and set arbitrarily at 65% of the maximum distance. This value provided a sufficiently irregular enlarged centroid to maintain the shape of the original cell, whilst at the same time compensated for any irregularity of the lines of the boundary (Fig. 2). The next step analyzed the intensity of the cell measured in concentric regions. The intensity values of every equidistant ring, based on the previously calculated centroid were averaged to create an intensity profile. The values of the profile were low-pass filtered to remove the rapid variations of intensity. Whilst the profiles varied considerably from cell to cell, all presented one common characteristic: as the profile approached the boundary of the cell, a minimum value was followed by a maximum (Fig. 3). The location of this minimum value was related to a drop in intensity towards the boundary of the cell and was used to determine the location of the outer ring (Fig. 4).

The region of the focal adhesions of interest, i.e. the cell periphery, was defined between the line of the outer ring and the boundary of the cell. Once the cell periphery calculated, the focal adhesions were segmented in the following way.

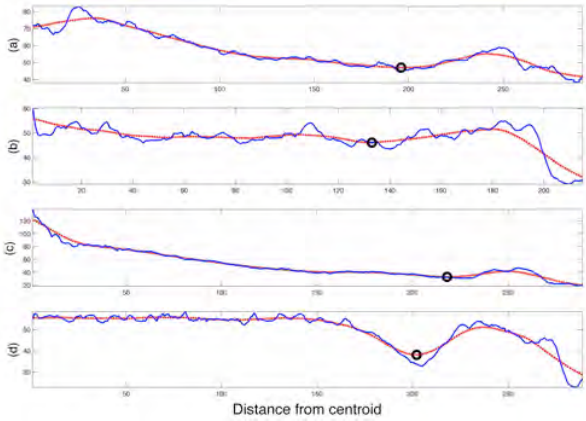

Fig. 3. Intensity profiles of the average intensity of concentric rings based on the irregular centroids (Fig. 2). The solid blue line is the actual average intensity and the red dashed line is a smoothed version. The last minimum value (from the centroid) before a maximum was used to determine the location of the outer ring.

Single [1] or double [4] intensity thresholding techniques were unsuitable as the intensity of the pixels of the focal adhesions varied considerably with each cell. Therefore, regions of maximum intensity were obtained with a gradient calculation (Fig. 5a,c). These regions were used as seed points for a region-growing algorithm based on the modified version presented by Hojjatoleslami and Kittler [5]. The edges obtained with Canny's algorithm [6] (Fig. 5b,d) were used as the stopping-criterion of the region-growing algorithm. Finally, the regions of bright intensity that were segmented by the previous series of steps were considered as the focal adhesions of MEFs. A series of morphological measurements were obtained to test the statistical difference between the two groups.

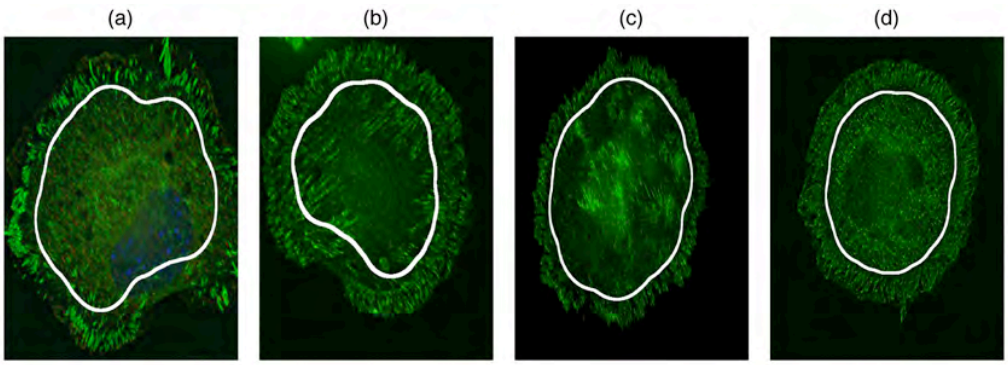

Fig. 4. The outer ring boundary overlaid on the original images. Notice how the outer ring is better located in some cells (a, c, d) than others (b). This is due to the nature of the cell in terms of shape and intensity distribution.

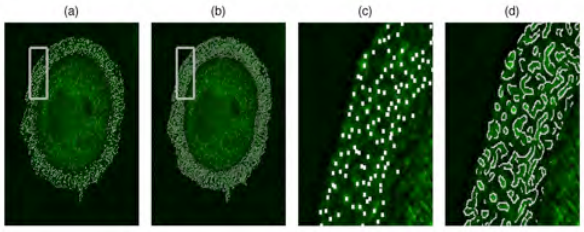

Fig. 5. Illustration of the region of maxima and edges for one cell (Fig. 1d). (a) Regions of maxima, (b) edges, (c) ROI from (a), (d) ROI from (b).

In addition to the number of focal adhesions (1), the following measurements were calculated for the segmented focal adhesions: (2) average area, (3) average eccentricity, (4) average major axis/minor axis, (5) focal adhesions density (objects within the cell periphery), (6) focal adhesions density (focal adhesion area within the cell periphery), (7) average intensity of the focal adhesions, (8) average intensity of the background (pixels that were not focal adhesions), (9) average intensity of the outer ring. Student's t-tests were used to compare the two groups.

All the image processing and statistics were performed using Matlab®.

3. RESULTS

The focal adhesions of the four representative images are shown in Fig. 6. The results in Fig. 6a,b correspond to group A and Fig. 6c,d correspond to group B. From the images, it appears that the focal adhesions of group B are smaller than those of group A.

Two of the previous measurements showed statistical difference (average area, p=0.0093; average major axis/minor axis, p=0.0365) between the groups using a two-sample t-test. Group A showed larger and more elongated lamellipodia than group B (Fig. 7a,b). Independently of these results, a manual delineation of the adhesions was performed. The delineation measured the length of focal adhesions at cell peripheries, discarded adhesions that crossed each other and priority was given to longer and straighter adhesions. The length of group B was on average 70% of that of group A with $p<0.001$, which confirms the automatic results. A sensitivity analysis to the Euclidean distance that was set at 65% was performed (Fig 7c) which showed the variation of the p-value to the range between 30-80%

4. DISCUSSION

The algorithm described here is totally automatic and does not require any tuning of parameters. The present work exploits the characteristics of the focal adhesions on travelling MEFs, namely, the intensity of the focal adhesions themselves, and the distribution of these along an external ROI that is visually distinct from the inner region of the cell. This inner region can have varied characteristics in terms of intensity, it can be uniformly bright or dark, it can have a bright center and decrease intensity towards the boundary or it can have a random distribution. However, in all cases, there is a ring with dark intensity before a region of high intensity towards the boundary of the cell. This region is called in this work "the outer ring" and was used together with the external boundary of the cell to locate the cell periphery.

As it can be observed from Figs. 3 and 4, the precise location of the outer ring depends on how well defined are the profiles, while Fig. 4d presents a very sharp and clear location of the outer ring, Fig. 4b is not as well located and its location could be inferior to one traced manually by an experienced user. On the other hand, the advantage of processing a large number of images automatically without inter- and intra-observer variability has considerable advantages over manual processing.

The sensitivity analysis of Fig 7c was interesting as it was clear that the area of the lamellipodia was not sensitive to the variation, as opposed to the ratio of the major to minor axes. In future work we consider that a more thorough morphological analysis [7] of the focal adhesions, the cell periphery, the outer ring and the shape of the cell. In addition, the algorithm should be tested with more images as the samples were relatively small. This analysis will also focus on the robustness of the measurements.

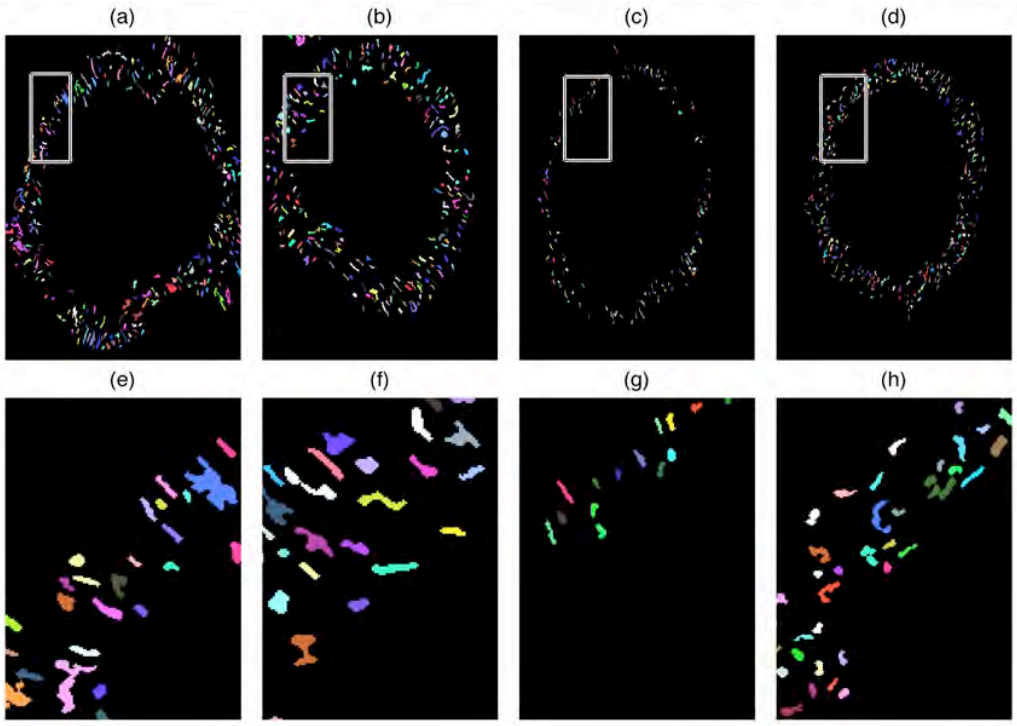

Fig. 6. (a-d) Segmented focal adhesions for the cells of Fig. 1. The white box indicates ROIs that are displayed in (e-h). Focal adhesions are labeled with random colors for visualization purposes.

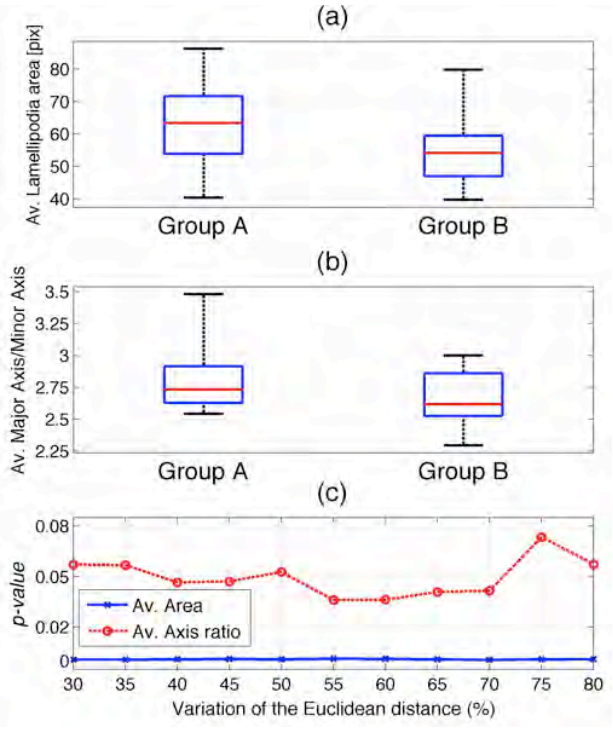

Fig. 7. (a,b) Boxplots of two measurements extracted from the focal adhesions. Both cases are statistically different with $p<0.05$. (c) Sensitivity analysis to the parameter of the variation of the Euclidean distance.

5. REFERENCES

[1] N. Otsu, "A Threshold Selection Method from Gray-Level Histograms," *IEEE Trans. Syst. Man Cybern.*, vol. 9, no. 1, pp. 62–66, Jan. 1979.

[2] J. Serra, "Introduction to mathematical morphology," *Comput. Vis. Graph. Image Process.*, vol. 35, no. 3, pp. 283–305, Sep. 1986.

[3] H. Samet and M. Tamminen, "Efficient component labeling of images of arbitrary dimension represented by linear bintrees," *IEEE Trans. Pattern Anal. Mach. Intell.*, vol. 10, no. 4, pp. 579–586, Jul. 1988.

[4] K. M. Henry, L. Pase, C. F. Ramos-Lopez, G. J. Lieschke, S. A. Renshaw, and C. C. Reyes-Aldasoro, "PhagoSight: an open-source MATLAB® package for the analysis of fluorescent neutrophil and macrophage migration in a zebrafish model," *PloS One*, vol. 8, no. 8, p. e72636, 2013.

[5] S. A. Hojjatoleslami and J. Kittler, "Region Growing: A New Approach," *IEEE Trans. Image Process.*, vol. 7, pp. 1079–1084, 1995.

[6] J. Canny, "A computational approach to edge detection," *IEEE Trans. Pattern Anal. Mach. Intell.*, vol. 8, no. 6, pp. 679–698, 1986.

[7] C. C. Reyes-Aldasoro, L. J. Williams, S. Akerman, C. Kanthou, and G. M. Tozer, "An automatic algorithm for the segmentation and morphological analysis of microvessels in immunostained histological tumour sections," *J. Microsc.*, vol. 242, no. 3, pp. 262–278, Jun. 2011.